

Magnetic force-induced damping effect for magnetic bearing motor

Chien-Chang Wang, Y. D. Yao, Yu-Hsiu Chang, Pi-Cheng Tung, and Ren-Bin Xiao

Citation: [Journal of Applied Physics](#) **97**, 10Q502 (2005); doi: 10.1063/1.1847251

View online: <http://dx.doi.org/10.1063/1.1847251>

View Table of Contents: <http://scitation.aip.org/content/aip/journal/jap/97/10?ver=pdfcov>

Published by the [AIP Publishing](#)

Articles you may be interested in

[Comparison of electromagnetic performance of brushless motors having magnets in stator and rotor](#)
J. Appl. Phys. **103**, 07F124 (2008); 10.1063/1.2838222

[Design considerations of electromagnetic force in a direct drive permanent magnet brushless motor](#)
J. Appl. Phys. **103**, 07F117 (2008); 10.1063/1.2835480

[Prediction and analysis of magnetic forces in permanent magnet brushless dc motor with rotor eccentricity](#)
J. Appl. Phys. **99**, 08R321 (2006); 10.1063/1.2165595

[Development of micromagnetic bearing motors with suppressed magnetic coupling effect for small form factor optical drives](#)
J. Appl. Phys. **99**, 08R302 (2006); 10.1063/1.2150387

[Analysis of magnetic forces in magnetically saturated permanent magnet motors by considering mechanical and magnetic coupling effects](#)
J. Appl. Phys. **91**, 6976 (2002); 10.1063/1.1456397



Re-register for Table of Content Alerts

Create a profile.



Sign up today!



Magnetic force-induced damping effect for magnetic bearing motor

Chien-Chang Wang

Materials Science and Engineering, National Chiao Tung University, Hsinchu 300, Taiwan

Y. D. Yao^{a)}

Institute of Physics, Academia Sinica, Taipei 115, Taiwan

Yu-Hsiu Chang

Optoelectronics and Systems Laboratories, Industrial Technology Research Institute (ITRI), Hsinchu 310, Taiwan

Pi-Cheng Tung and Ren-Bin Xiao

Mechanical Engineering, National Central University, Taoyuan 320, Taiwan

(Presented on 11 November 2004; published online 17 May 2005)

An innovative damping induced by magnetic force was designed successfully for a totally passive magnetic bearing motor. A magnetic ring of high permeability and an annular-shaped rubber pad were mounted on the stator 0.55 mm below the permanent magnet of the rotor. Computer simulations were compared with experimental measurements to decide on the material and configuration of the critical components. The natural frequencies for lateral and rotational modes of the rotor are around 22 Hz measured by impulse method. Both the magnetic bearing motor with and without magnetic damping are rotated at a rated speed of 3840 rpm, which is far above the first critical speed of 1305 rpm. Without magnetic damping, the natural damping ratio in the radial direction of the rotor is 0.0655. After damping, it increases to 0.1401. We have demonstrated by both experimental measurement and theoretical calculation that the antishock performance is significantly improved by the innovative damping technology in a passive magnetic bearing motor. © 2005 American Institute of Physics. [DOI: 10.1063/1.1847251]

I. INTRODUCTION

Passive magnetic bearing^{1,2} is one of the solutions to achieve low noise and long life span of the spindle motors that are applied in the data storage disk drives, such as hard disk drive (HDD) and digital versatile disk (DVD) devices. However, the magnetic bearing system has a disadvantage that is a lack of damping. Therefore, in the spindle motor systems which support on these bearings can be expected likewise to show very small damping. This condition is revealed by very large amplitudes as rotors transverse their critical speeds, great sensitivity to unbalanced conditions, and poor resistance to instability. There are some methods³⁻⁵ for introducing damping into passive magnetic bearing systems by using a resilient material. In general, these configurations rely on constructing an intermediate housing that is supported by a ball between the rotor and stator. The damping material is positioned between the housing and the stator. The housing adds to system complexity and causes a reduction in the resonant frequency. In addition, the stiffness and damping are coupled. In this study, an innovative damping induced by a magnetic force is investigated for the magnetic bearing motor systems.

II. DESIGN AND SIMULATION

Figure 1 shows the configurations of the magnetic bearing motor. The ratio of slot number to pole number is 4:4. The radial air gap between the stator and the rotor was fixed

to 7×10^{-4} m. A Ba-ferrite ring with an inner diameter of 3.14×10^{-2} m, axial length of 1.34×10^{-2} m, and outer diameter of 3.94×10^{-2} m was used for the magnetic rotor. Outside of the Ba-ferrite ring, an iron yoke with an outer diameter of 4.1×10^{-2} m was attached. The magnetic bearing spindle motor was designed under the conditions of the rated speed which is 3840 rpm. Two permanent magnetic annular magnetic rings were mounted on a shaft and two annular magnetic rings were mounted on a stator. The shaft bottom contacted the thrust plate. The magnet geometry has been optimized in order to increase the restoring force in the radial direction. NdFeB magnets with $(BH)_{\max}$ of 45 MGOe were used. The dimensions of the rotating and stationary magnets are as follows. The OD of the rotating magnet is 6×10^{-3} m and the ID is 3×10^{-3} m. The stationary magnet OD is 1×10^{-2} m and ID is 7×10^{-3} m. The thickness of magnet used in both rotor and stator is 4×10^{-3} m. The ro-

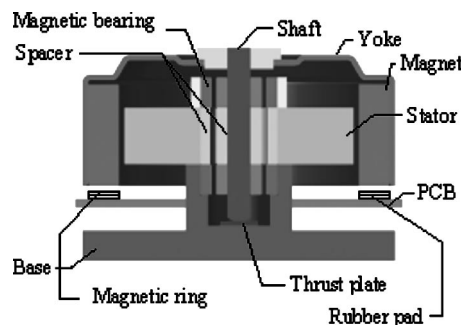


FIG. 1. Magnetic bearing motor.

^{a)}Electronic mail: ydyao@phys.sinica.edu.tw

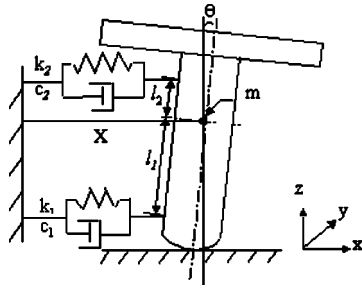


FIG. 2. The simplified physical model of the magnetic bearing motor system.

tating and stationary magnets had a slight 5×10^{-4} -m radial air gap. Both rotating and stationary magnets had the same magnetization direction along the axial axis. The axial distance between upper magnetic bearing and lower one is 7.5×10^{-3} m.

In order to improve the damping of the magnetic bearing motors, a configuration has been designed. The damping device is comprised of a magnetic ring with high permeability and an annular rubber pad (the damping is 0.2 N s/m), which is attached to the stator. It has the same outer and inner diameters with the permanent magnet of the motor and is 0.55 mm below it. The undesired rotor vibration forces are transmitted from the rotor permanent magnet through the magnetic field. The resistance of the rubber pad to the vibrations results in frictional forces, thus dissipating the vibration energy.

The damping ratio ξ is chosen as an index to evaluate the improvement of the damping. The static state of the rotor is considered. To carry out the analytic analysis easily, the simplified model is assumed, as shown in Fig. 2. It shows that the rotor is supported by two magnetic bearings. Suppose that the rotor can do the translation and rotation motions in only one degree of freedom. The damping can be adjusted by varying the material of the rubber pad and the thrust plate is frictionless. Refer to Newton's second law, a mass distribution m , the equation of motion is as follows:

$$mx + (k_1 + k_2)x + (k_2l_2 - k_1l_1)\theta + (c_1 + c_2)x + (c_2l_2 - c_1l_1)\theta = 0, \tag{1}$$

$$J\theta + (k_2l_2 - k_1l_1)x + (k_2l_2^2 + k_1l_1^2)\theta + (c_2l_2 - c_1l_1)x + (c_1l_1^2 + c_2l_2^2)\theta = 0. \tag{2}$$

Each of the two magnetic bearings is linked to an elasticity and damping parameter k and c , respectively, with indices 1 and 2. The l_1 and l_2 represent the length from the position of the center of mass to the lower and upper magnetic bearings. The x denotes the displacement for the simplified case of translation displacement along the X axis. θ is the angle of the rotor rotated about the center of mass position relative to the Y axis.

Finite element analysis (FEA) was used to analyze the magnetic force of the magnetic bearing motor. Approach to this computation of radial force of the development system, the stator was fixed and the rotor was shifted along the positive X axis as the following five different positions, 0, 1

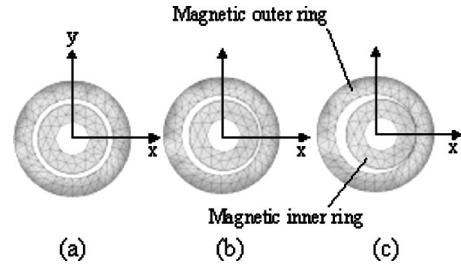


FIG. 3. 2D top view of relative location of the rotor and stator.

$\times 10^{-4}$, 2×10^{-4} , 3×10^{-4} , 4×10^{-4} , and 4.9×10^{-4} m. Three relative positions of magnetic inner and outer rings were shown in Fig. 3. Figure 3(a) shows no radial displacement of the rotor along positive X axis. The displacement of the rotor along positive X axis is 3×10^{-4} m in Fig. 3(b). Figure 3(c) shows a radial displacement of the rotor along positive X axis of 4.9×10^{-4} m. Since the radial force was known, then the radial stiffness of 1288 N/m of the magnetic bearing is perfectly determined.

III. EXPERIMENTAL TESTING

For measuring the damping ratio, a miniature hammer is included in this testing system. When magnetic motor was in its static state, an accelerometer was attached to the rotor in the radial direction. The hammer gave an impact shock in the radial direction of the rotor as the input driving force and the rotor of the magnetic bearing motor was excited and vibrated. The radial acceleration of the rotor was measured by using the accelerometer and the time response of the rotor was recorded. By using the fast Fourier transform (FFT), the frequency domain of the radial runout could be obtained. From the frequency impulse method the damping ratio ξ was calculated by the general equation, $\xi = \delta / \omega_n \tau_d$. The δ was equal to $\ln(x_1/x_2)$, where the x_1 and x_2 were the peak amplitudes chosen from the time response profile.

IV. RESULTS AND DISCUSSION

Figure 4 shows the time response and frequency response without the damping device from the experiment. Without the damping device, the measured damping ratio is 0.0655. From the experimental data it indicates that the natural frequency of original magnetic bearing motor is 23.5 Hz.

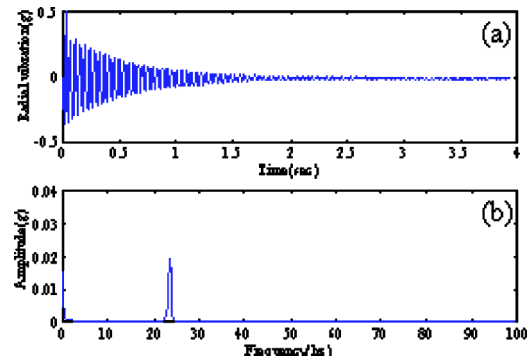


FIG. 4. (a) Time response and (b) frequency response without damping device.

To perform the calculation of the damping ratio with the damping device, the values of parameters as follows are considered. Damping $c=0.2$ N s/m was chosen, $l_1=7.85 \times 10^{-3}$ m, $l_2=3.65 \times 10^{-3}$ m, $c_1=c_2=0.2$ N s/m, $k_1=k_2=1288$ N/m, and $m=7.1 \times 10^{-2}$ kg. Then the differential equations (1) and (2) were solved. According to the same parameters that are used in the analytical analysis, the experiment was performed. The damping ratio of the experimental and analytical model is 0.1401 and 0.1170, respectively. It has the same significant levels of passive radial damping.

Both the results obtained from the two methods in the damping ratio are greater than 0.1. The corresponding natural frequencies are 21.75 and 19 Hz, respectively. It has the same agreement with the damping ratio and the natural frequency. The system resonance is avoided. Because the rated speed is around 64 Hz and the experimental and analytical model data in natural frequency are 42.25 and 45 Hz below 64 Hz, respectively. Figure 5 shows the time response and frequency response with the damping device from the experiment. The damping device applied in the developed magnetic bearing system, the ratio in the damping ratio of our device to the original device is 214%.

V. CONCLUSION

The damping device is applied in the developed magnetic bearing system and the ratio in the damping ratio of our device to the original one is 214%. The natural frequencies for lateral and rotational modes of the rotor are around 22 Hz measured by the impulse response method. It is 42 Hz below the rated speed of 64 Hz, therefore, the system resonance is

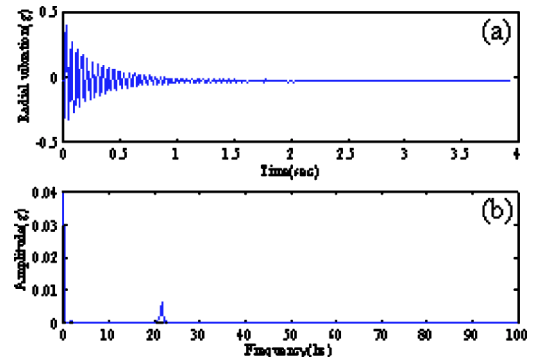


FIG. 5. (a) Time response and (b) frequency response with damping device.

avoided completely. Finally, we have demonstrated that the antishock performance is significantly improved by our innovative damping technology in a passive magnetic bearing motor which will be useful for high-density data storage applications.

ACKNOWLEDGMENTS

Financial support of the National Science Council through the project NSC 92-2120-M-001-008 and from the main research project of Academia Sinica are gratefully acknowledged by the authors.

¹J.-P. Yonnet, IEEE Trans. Magn. **14**, 803 (1978).

²J.-P. Yonnet, IEEE Trans. Magn. **17**, 1169 (1981).

³A. Tozune, Electric Power Applications, IEE Proceedings B (1991), Vol. 138, p. 21.

⁴H. Lotz, U.S. Patent No. 5,910,695 (1999).

⁵J. Imlach, U.S. Patent No. 6,448,679 (2002).